American Mineralogist, Volume 87, pages 1273–1278, 2002

Atomic-scale observations of franckeite surface morphology

RENÉ B. HENRIKSEN,[1] EMIL MAKOVICKY,[1] S.L.S. STIPP,[1,*] CAMILLA NISSEN,[1] AND CARRICK M. EGGLESTON[2]

[1] Geological Institute, Copenhagen University, Øster Voldgade 10, DK-1350 Copenhagen K, Denmark
[2] Department of Geology and Geophysics, University of Wyoming, Laramie, Wyoming, 82071-3006, U.S.A.

ABSTRACT

Franckeite, approximately $Pb_{4.6}Ag_{0.2}Sn_{2.5}Fe_{0.8}Sb_2S_{12.6}$, consists of alternating pseudohexagonal (H) and pseudotetragonal (Q) layers. Scanning tunneling microscopy (STM) and atomic force microscopy (AFM) of freshly cleaved franckeite, from San José, Bolivia, revealed the atomic structure of the pseudohexagonal component. On AFM images, the expected pattern with b = 3.2 Å was observed. STM revealed a ÷3 ¥ ÷3 superstructure, with b' = 6.3 Å, interpreted to be caused by tunneling effects. The pseudotetragonal layer was not identified in any images.

Layer modulation, which results from the non-commensurate fit of the alternating H and Q layers, was observed with both AFM and STM. Modulation waves are sinusoidal and regular and they are always parallel. The calibrated modulation wavelengths averaged to 3.77, 4.10, 4.45, and 4.74 nm (with uncertainty £0.10 nm) corresponding to pseudotetragonal/pseudohexagonal (Q/H) matches of 13/12, 14/13, 15/14, and 16/15, respectively. These correspond with observations made using bulk analytical methods on individual members from the franckeite-cylindrite family but scanning probe microscopy (SPM) was able to show that Q/H match varies on a local scale, with sharp domain boundaries. Domains can be on the order of 150 nm in width.

INTRODUCTION

Franckeite belongs to a family of complex sulfide minerals where substitution results in a range of complicated structures, making them a fascinating topic of study from the mineralogic perspective. Electron-sharing, particularly in some crystallographic orientations, causes most members of the family to be semi-conducting, which makes them of interest to materials scientists. Bulk structural parameters have been determined for a number of them from X-ray diffraction (XRD) and transmission electron microscopy (TEM) but the averaging inherent with macroscopic techniques may obscure local variations in structure and composition. The purpose of this study was to use scanning probe microscopy, which has angstrom-scale resolution, to observe local atomic structure on cleaved surfaces of one member of the sulfosalt family.

Franckeite has approximate composition: $Pb_{4.6}Ag_{0.2}Sn_{2.5}Fe_{0.8}Sb_2S_{12.6}$ (Organova et al. 1980). It is semi-conducting in the direction perpendicular to cleavage and is composed of alternating pseudohexagonal (H) and pseudotetragonal (Q) layers, where H-layers have an *A*-centered subcell with b = 3.68 Å, c = 6.32 Å, a = 91° and the Q-layers have an *A*-centered pseudotetragonal subcell with b = 5.84 Å, c = 5.90 Å, a = 91° (Wang 1989). The layers are stacked HQHQ along **a** with a periodicity of 17.3 Å but they are non-commensurate (Makovicky and Hyde 1992). The misfit in the match of the Q and H subcells induces a structure modulation along **c**. The wavelength (l), or distance between the modulation highs, varies as a function of chemical composition, especially as a function of the Pb^{2+}/Sn^{2+} ratio (Makovicky and Hyde 1992). Reported wavelengths vary from ~39 to ~47 Å corresponding to a range of Q/H matches from 14Q/13H in bulk samples of Pb-free franckeite to 16Q/15H for natural franckeite specimens (Organova et al. 1980; Kissin and Owens 1986; Li et al. 1988; Williams and Hyde 1988; Wang 1989; Wang and Kuo 1991). Demonstration of the existence of local variation in wavelength, thus in the match parameters, and determination of a relative scale for a coherent domain size have not yet been possible with classical mineralogical methods.

Scanning probe microscopy (SPM) uses the highly local interactions between a sharp tip and the atoms of a surface to create a two-dimensional map where the physical property that the probe measures is represented as the third dimension. The sample is moved with respect to the tip by a piezoelectric element which can be scanned laterally and vertically in sub-angstrom increments allowing atomic-scale resolution. Details of the technique, image interpretation, and applications to other geological samples are presented in Eggleston (1994). Descouts and Siegenthaler (1992) offer abundant examples of the application of SPM techniques to a wide variety of surfaces. In scanning tunneling microscopy (STM), the probe is a conductive wire, which is brought close to a sample surface. A voltage bias on the sample induces a measurable tunneling current to flow between the tip and a conducting or semi-conducting surface. Resulting images represent the spatial variation in electronic structure over the atomic array. In atomic force

* E-mail: stipp@geol.ku.dk

0003-004X/02/0010–1273$05.00

microscopy (AFM), a tip is mounted on a cantilever that has a very light spring constant, so variation in the atomic-scale forces over the surface causes repulsion or attraction. Although there are many forces contributing, the most influential is often simply hard-sphere repulsion between atoms of the tip and the sample so the resulting image is a map that approximates topography (Stipp et al. 1994). AFM and STM probe different physical properties of a surface, so their images offer different kinds of information, and comparison of the images often offers new information about surface behavior.

MATERIALS AND METHODS

Natural samples of franckeite from San José, Bolivia were cleaved in air with a scalpel along (100) cleavage planes. The samples were mounted on steel sample holders with double sided tape, acrylite, or silver paint.

We used a Digital Instruments (DI) multi-mode scanning probe microscope. This instrument is designed so that the sample sits on the piezoelectric element and the tip is held stationary above the surface. The sample is rastered forward and back along the **x**-direction as **y** is sequentially incremented. Thus **x** is called the "fast-scan direction" and **y**, the "slow-scan direction." We used STM tips cut from Pt/Ir wire with wire cutters and various bias/set point combinations. For AFM, we used standard Si_3N_4 cantilevers with an integrated pyramidal tip and a spring constant of approximately 0.12 N/m. All images were collected in air. Humidity in the laboratory ranged from 30 to 60% and temperature from 18 to 28 °C during the days of the experiments. Experience has shown that water vapor from air forms a capillary layer between tip and sample (Stipp et al. 1996), making force determinations in air meaningless, but for these studies, force was maintained as low as possible by periodically ramping set point as far as tip withdrawal, then engaging again and adjusting set point to a value just below tip lift-off. Minimizing force in this way minimizes contact area and friction, thus significantly decreasing the extent of multiple tip imaging. Specific imaging conditions are reported in the caption for each figure. We collected scores of images from a number of sub-samples of the frankeite sample and we applied standard SPM practice for avoiding artifacts. All images were flattened using a linear fit and those presented here are either raw data or lightly low-pass filtered so as to remove high frequency noise. Flattening, covariance, and two-dimensional Fourier transform treatment of the data were made with the DI software provided with the microscope. Interpretations based on low-pass filtered images were verified by careful examination of raw data.

RESULTS AND DISCUSSION

Atomic scale structure and superstructure

On flat, freshly cleaved samples of franckeite, atomic-scale images could be collected with both AFM and STM (Figs. 1 and 2). The images appear slightly distorted. Hexagons are stretched or compressed and the angles between rows of atoms are not the expected 120°, making it difficult to directly determine whether the particular franckeite surface examined was a Q or H layer. Distortion is a pervasive artifact in SPM. It is relatively common to see hexagons stretched to appear as monoclinic or even as orthorhombic or tetragonal arrays, and cubic surfaces can be distorted to appear monoclinic or hexagonal. It is especially easy to recognize distortion when sequential images, which are collected as the scanner moves first in the "up" (+**y**) and then in the "down" (–**y**) scan-directions, differ in appearance. Distortion is explained by an unwanted movement of the tip with respect to the sample, which is separate from the expected scanning motion. It is often called "thermal drift" but recent experiments prove that distortion bears no relation to changes in temperature, as such. Rather, it results from nonlinear instrument response, especially during the first hour after the instrument is turned on (Henriksen and Stipp 2002).

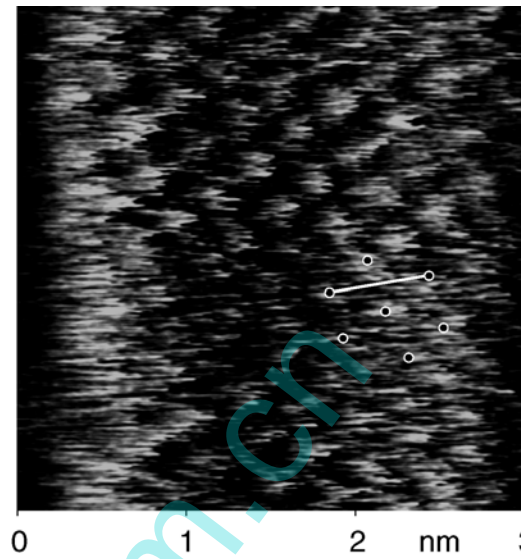

FIGURE 1. Height mode AFM image of the (100) surface of franckeite. Scan rate was 24 Hz and force was held as low as possible while maintaining contact. The "edge effect" at the left side of the image results as the tip begins each new scan line. Light spots represent areas that are topographically higher. "Drift" has distorted the hexagonal atomic pattern (shown as black dots in white circles), but the distance marked nearly along **x** (white line) is 6.1 Å, which is within uncertainty limits of expected atomic separation along the **c** axis.

In general, angles in SPM images cannot be trusted unless a method is adopted to rigorously account for distortion; distances must be carefully determined to minimize distortion effects. "Drift," one of the components of distortion, is at a minimum along the fast-scan (**x**) direction. "Scaling," the second component, is at a minimum if the piezoelectric scanner was calibrated after more than an hour warm-up time and at the instrument conditions intended for scanning (Henriksen and Stipp 2002). Thus, for determining atomic spacings in this study, we measured average distances in the fast-scan direction from the two-dimensional Fourier transforms of the images. Figure 1 shows a typical AFM image. Although the pattern appears shortened in the slow-scan (**y**) direction, atomic spacings in a line as close to the **x**-direction as possible, are consistent with the pseudo-hexagonal layer.

Figure 2a is typical of the STM images. A hexagonal pattern is also apparent, but the dimensions measured indicate that the spacing represents a ÷3 ¥ ÷3 superstructure (Fig. 2c). Su-

perstructures can result when a surface relaxes after cleavage. Bonding forces are no longer balanced as they were within the bulk so some atoms shift position slightly up or down from the atomic plane, making them appear in the image as brighter (higher) or weaker (lower) spots than they would otherwise be. Another mechanism for producing a superstructure is the overlapping of electron clouds from more than one crystal layer, so that tunneling is enhanced in certain directions. In scores of images, we never saw superstructure with AFM, but we did by STM, so we can interpret that the superstructure on franckeite surfaces is not caused by true relative difference in atom height, but rather, that electronic overlap of the top layer with the underlying structure results in stronger tunneling at some positions. The nodes of enhanced tunneling which form the superstructure coincide with the nodes of the first (approximate) match of *A*-centered Q and H subcells in the franckeite structure: $2b_Q \approx 3b_H$ and $c_Q \approx c_H$. This coincidence lattice is not centered as such. Because of the match of the b_Q/b_H subcell, however, the Q layer below each H layer can occur with equal probability in two positions. These are separated by a distance of 0.5 $b_{Q\,(subcell)}$ and produce the centration point of the observed ÷3 ¥ ÷3 lattice, which is fully equivalent to its (0, 0, 0) node in the layer stack. An alternative explanation, that these positions represent an ordering of minor cations in the H layer, is unlikely. This would result in observation of periodicity in the X-ray and HRTEM studies, but this has not been observed (Williams and Hyde 1988). Tunneling enhancement in the layer stack is the most attractive explanation for the observed superstructure. Because imaging is most effective using negative bias voltage, we interpret that tunneling occurs through negatively charged sites, that is, the sulfur atoms.

The vertical distance separating the top of adjacent H layers is ~17.3 Å; that separating the top of the H layer from the top of the next Q layer is ~6 Å. Both STM and AFM are capable of imaging steps of this height at atomic resolution, so we looked for evidence of a step where we could see atomic spacing on both H and Q layers. From the proportionality of Q and H layers in franckeite, we would expect to be able to see pseudotetragonal surfaces as well. However, in all experiments, with both STM and AFM, the images that we obtained were consistent with the pseudohexagonal spacing. We cannot say why we were unable to image the Q layer. It seems not to be a matter of differences in semi-conducting properties of the two layers, i.e., in the ease of tunneling, because AFM was similarly ineffective at imaging the pseudotetragonal layer. It is possible that during cleavage, the H layer relaxes to a smooth surface that is easy to image, whereas the Q layer becomes rough and unrecognizable as an atomic array.

Modulation

Modulation is characteristic of this sulfosalt family of minerals and its spacing or wavelength varies with chemical composition. It was observable with both AFM and STM. Ridges and troughs are always straight and parallel; bending was never observed (Fig. 3a). Cross-sections of STM images, such as Figure 3b, show a sinusoidal oscillation representing the interaction between clouds of electrons at the tip and sample, but it can be argued that STM images, which represent electron density, are not a true picture of topography. AFM images are a closer representation of height. Figure 4 shows modulation imaged with AFM. The sinusoidal cross-section (Fig. 4b) has rounded tops but the valleys are slightly v-shaped. This is explained by the interference of the tip's profile with the modulation. The AFM tip can ride over the modulation tops, tracing

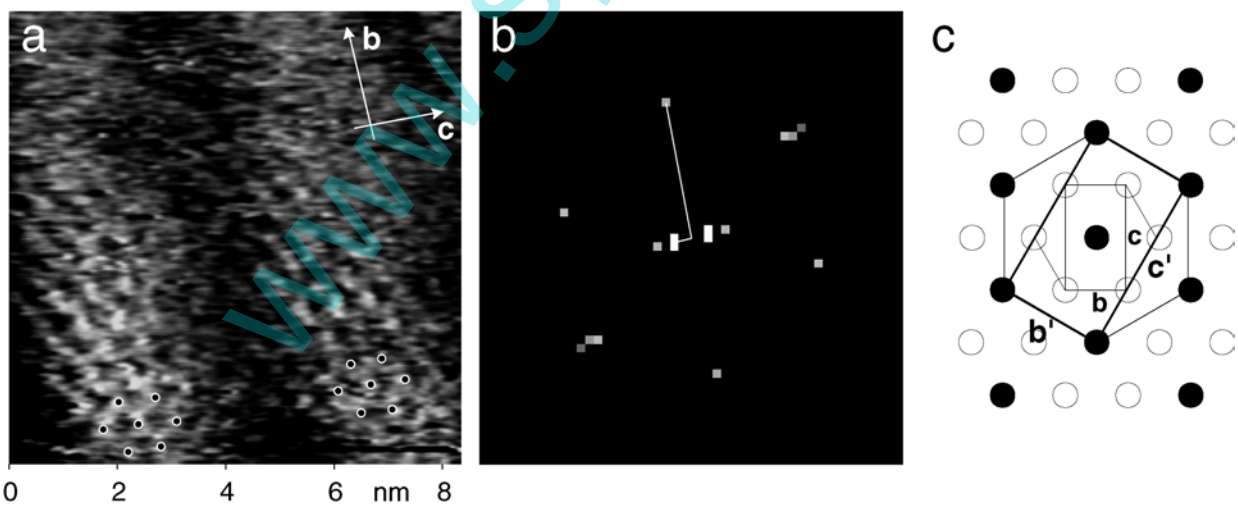

FIGURE 2. (**a**) Height mode STM image of the (100) surface of franckeite. Scan rate was 30 Hz; setpoint, 400 pA; bias voltage, –900 mV. Brighter spots represent sites of enhanced tunneling. The slightly distorted hexagonal patterns (marked by black dots in white circles) have separation distances along the fast-scan, **x**-direction of about 6.3 Å along *b*, instead of the expected 3.7 Å. This indicates ÷3 ¥ ÷3 superstructure. (**b**) Two-dimensional Fourier transform. The long vector from the origin (about 5.7 Å) represents the perpendicular distance between the atomic rows, which is approximately half the distance *c*; the short vector represents modulation spacing (37 Å). (**c**) A schematic diagram showing the basic hexagonal layer as open circles (with axes b = 3.7 Å and c = 6.3 Å) and its ÷3 ¥ ÷3 superstructure shown as filled circles (with axes b' = 6.3 Å, c' = 11.1 Å).

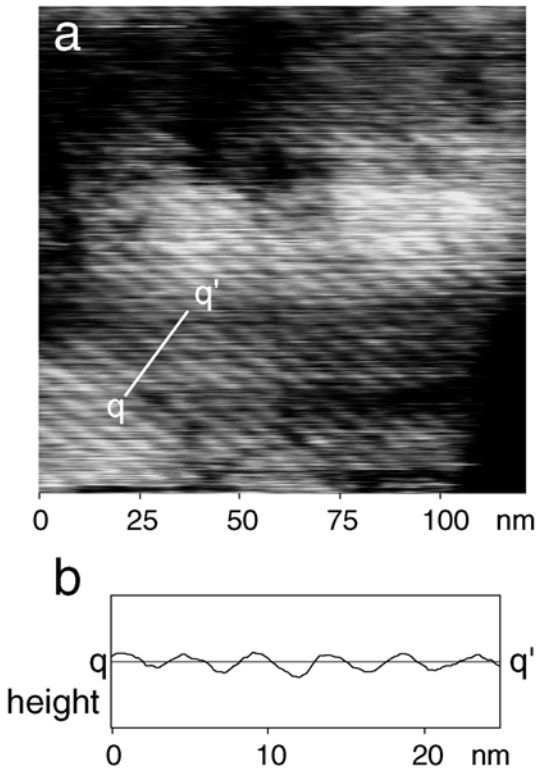

FIGURE 3. (**a**) Height mode STM image at lower resolution, showing modulation structure. Scan rate, 10 Hz; set point, 400 pA; bias 795 mV. Modulations are parallel, with no bending observable. (**b**) Cross-section (averaged profile) perpendicular to the modulation direction indicates a sinusoidal waveform.

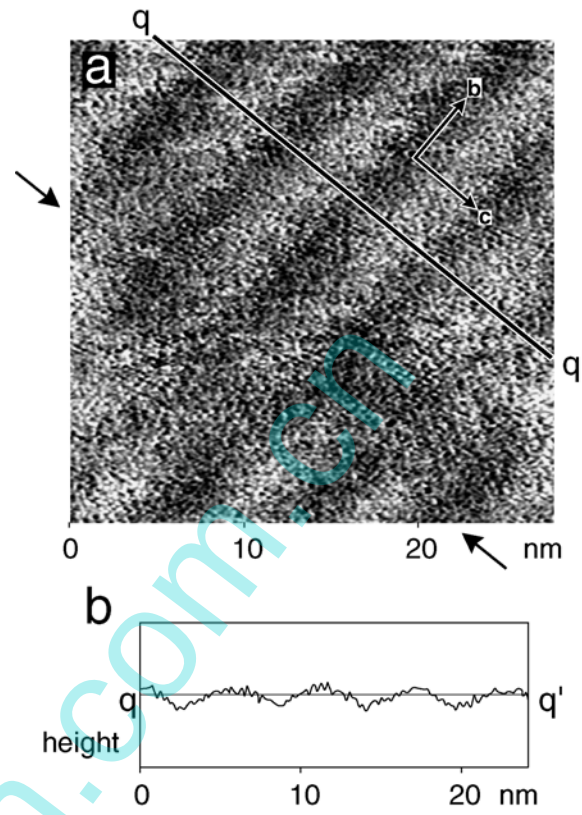

FIGURE 4. (**a**) Height mode AFM image taken at 5 Hz. (**b**) The cross-section is sinusoidal with slight v-shaped valleys resulting from interference of pyramidal tip shape with the edges of the modulation hollows. On the lower left corner of image (**a**), there is a different modulation spacing separated by a feature that runs at an angle to the scanning direction (between arrows). It represents a boundary between domains with different Q/H match: 14/13 in the upper right, 16/15 in the lower left, suggesting local differences in composition.

their real outline, but it is wider than the valleys so it cannot reach their bottoms and its edges get caught on the sides. The AFM and STM data together, however, strongly suggest sinusoidal modulation. This is consistent with high resolution TEM observations for franckeite (Williams and Hyde 1988) and for cylindrite (Makovicky 1976).

Modulation amplitude determined from AFM images varied considerably because corrugation recorded on atomic scale images is a function of scanning parameters, particularly scan-rate and gains. As the sample is scanned under the tip and the piezoelectric element attempts to respond to the detector feedback signal, there is not enough time for complete response before the next data are recorded. Thus, height is under-represented to varying degrees depending on how fast the sample is moving and what level of response rate has been set by the imaging parameters, so there is considerable uncertainty in measured modulation amplitudes.

One important question that we hoped SPM could answer concerned local variability in modulation wavelength. Unfortunately, distortion causes uncertainty in lateral distances measured. Although it is relatively easy to eliminate effects of drift and scaling by an Inverse Transform (Henriksen and Stipp 2002), for this work we were lucky because a number of the images recorded the atomic array at the same time as the modulation pattern (for example Fig. 4a). Average atomic distances for franckeite are well-defined from bulk experiments, so these images, where both atomic and modulation spacing were visible on two-dimensional Fourier Transforms, provided us with an excellent opportunity to use atomic spacing as an internal calibration, thus eliminating drift and scaling artifacts. We could precisely determine the orientation of the **c** axis to the modulation direction and we could measure the wavelength of the modulation structure in relation to the dimensions of the hexagonal subcell (m_i). In the direction normal to modulation ridges, the spacing between rows (b_i) was measured from the two-dimensional Fourier transform, such as is shown in Figure 5b. The ratio of b_i to the known bulk atomic spacing, b, for the H layer provided a conversion factor for determining true modulation spacing, $m = m_i(b/b_i)$ for that image.

In all of the images, wave propagation direction, that is the normal to the modulation ridges, was parallel to the **c** axis. This is consistent with XRD data for cylindrite (Makovicky 1976). The internally calibrated modulation wavelengths, all taken from sub-samples of the same franckeite specimen, are

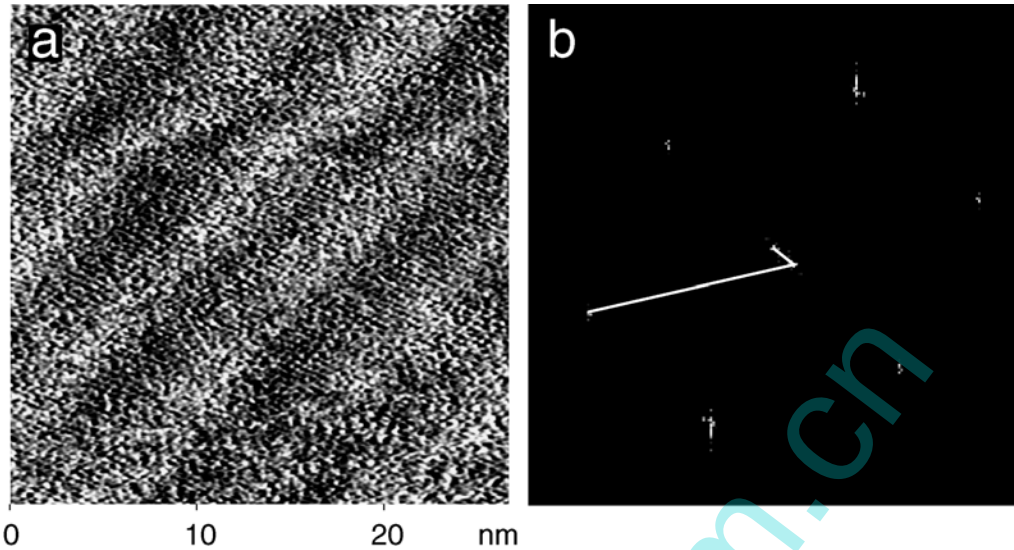

FIGURE 5. (**a**) Height mode AFM image taken at 5 Hz, flattened and low-pass filtered, where both modulations and atoms are resolved. (**b**) Two-dimensional Fourier transform, where the long vector represents atomic spacing, b_i, and the short vector, modulation spacing, m_i.

plotted in Figure 6. All of these local measurements fall into four groups of Q/H match: 13/12, which has previously been reported for bulk samples of cylindrite (Makovicky 1976); 14/13, reported for Pb-free bulk samples of franckeite (Li et al. 1988), 15/14 observed in bulk Pb-rich franckeite (Organova et al. 1980; Wang 1989), and 16/15, corresponding to a modulation spacing of 4.7 nm, reported for natural franckeite samples by Wang (1989). Note that uncertainty in Q/H match is less than ±0.10 nm, and the data separate themselves into discrete groups (Fig. 6). The variation in Q/H match within the same sample is significant because it demonstrates that domains with internally consistent structure coexist with neighboring domains with different, but internally consistent, Q/H match. This local variation implies that domains vary slightly in composition.

On one image (Fig. 4a), we were able to capture evidence of a change in modulation character on both sides of a linear feature running exactly perpendicular to modulation spacing and parallel to **c** (between arrows). The feature, however, cuts across the fast-scan direction, evidence that it is not likely an imaging artifact and it follows the direction expected for a domain boundary. As proof, Q/H mismatch on the top right is 14/13, and on the bottom left, 16/15, a difference in mismatch of two units. We note that in most cases, our random sampling of Q/H mismatch over the surface was not controlled, but a direct result of "drift," the relative (and uncontrollable) movement of the tip with respect to the sample. We took advantage of this annoyance and used the drift velocity, together with time lapse between capture of sequential images, to make a rough estimate of domain size. From sets of images where modulation spacing was known to differ, capture time and drift rate gave domain sizes on the order of 150 nm across.

Comparison with published work

Ma et al. (1997) studied a (100) cleavage surface of natural franckeite from Dachang, China, using a CSTM-9000 scanning tunneling microscope. They also obtained only images of the H layer, and reported average pseudohexagonal subcell dimensions b = 3.66 Å and c = 6.20 Å (with this precision),

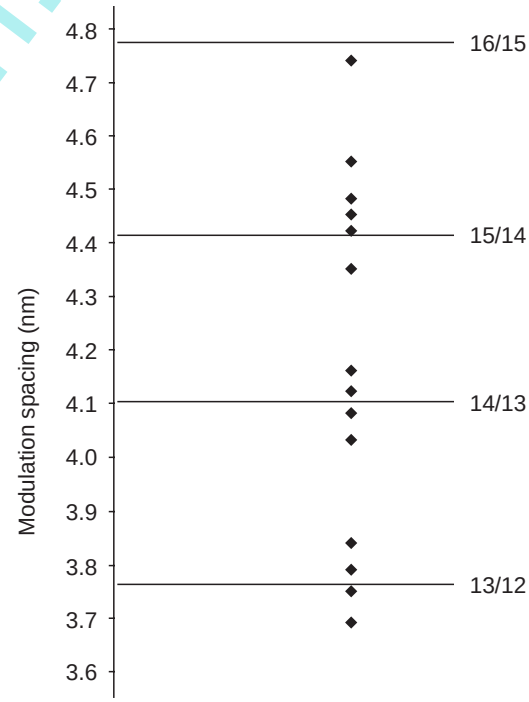

FIGURE 6. Modulation wavelengths measured from images (black diamonds) compare well to those calculated from Q/H match (horizontal lines). For Q/H match of 13/12, calculated modulation spacing is 3.77 nm, compared with the average of observed data, 3.77 ± 0.07 nm where uncertainty represents range in measurements. For 14/13, calculated is 4.10, observed average is 4.10 ± 0.07; for 15/14, calculated is 4.41, average, 4.45 ± 0.1 and for 16/15, calculated, 4.77, observed, 4.74 nm.

which are almost the same as the X-ray values of Wang (1989) from the same locality. The results of Ma et al. (1997) are at variance with our observations of the STM superstructure, but unfortunately, no comparison can be made between the two sets of data because distortion corrections have not been made, they do not report if they measured distances only along the fast-scan direction and their illustrations lack a recognizable scale. These researchers also claim to have measured two regular modulations perpendicular to each other, with average wavelengths of 69.8 Å and 47.0 Å, respectively. The latter value is identical to the modulations obtained by electron diffraction for Dachang franckeite by Wang et al. (1992). It also corresponds to the interlayer match of 16/15 given for this locality by Wang (1989). The images cited as evidence, however, depict the hexagonal substructure and comprise, at most, only half of one modulation wavelength; it is not clear from the article where the mistakes occurred.

Bengel et al. (2000) used STM and AFM to study the noncommensurate layer structure of the synthetic compound $[(Pb,Sb)S]_{2.28}NbS_2$. In this material, the pseudotetragonal layers are franckeite-like but the pseudohexagonal NbS_2 layers are trigonal-prismatic. This compound has only one-dimensional interlayer misfit, b_Q = 5.964 Å, b_H = 3.33 Å whereas the other dimension is common, c = 5.829 Å; the stacking direction of the triclinic structure is 17.649 Å. Layer geometry leads to quite a different layer match ($4b_Q \neq 7b_H$) and this was observed in their STM figures of the Q layer. No modulation of the pseudohexagonal layer was observed that would be analogous to our results.

Thus, our study revealed that: (1) the long-range modulation of the layered franckeite structure is regular over fairly extensive (100 to 1000 nm) domains; (2) the modulation vector has a simple crystallographic orientation, parallel to [001] of franckeite; (3) modulation follows a sine wave; (4) there are distinct modulation and compositional domains within a single franckeite sample; (5) a $\sqrt{3} \times \sqrt{3}$ superstructure is observed using STM but is absent during AFM imaging which can be explained by tunnelling through the closest approximate match between the H and Q layers; and (6) it is likely that tunnelling occurs through the negatively charged sites, that is, the sulfur atoms.

ACKNOWLEDGMENTS

We gratefully acknowledge O. Brogaard and T. Egeberg for technical support, B. Munch for help with drafting, and C. He for a last-minute translation of the Ma et al. article. Financial support was provided by The Danish National Research Council.

REFERENCES CITED

Bengel, H., Jobic, S., Moëlo, Y., Lafond, A., Rouxel, J., Seo, D.-K., and Whangbo, M.-H. (2000) Distribution of the Pb and Sb atoms in the (Pb,Sb)S layers of the franckeite-type misfit compound $[(Pb,Sb)S]_{2.28}NbS_2$ examined by scanning tunneling and atomic force microscopy. Journal of Solid State Chemistry, 149, 370–377.

Descouts, P. and Siegenthaler, H. (1992) Ten Years of STM. Proceedings of the 6th International Conference on Scanning Tunneling Microscopy, Interlaken, Switzerland. 12–16 August 1991, European Physical Society, North-Holland, 1703 p.

Eggleston, C.M. (1994) High resolution scanning probe microscopy: Tip-surface interaction, artifacts, and applications in mineralogy and geochemistry. In Clay Minerals Society Workshop Lectures, 7, 1–90.

Henriksen, K. and Stipp, S.L.S. (2002) Image distortion in scanning probe microscopy. American Mineralogist, 87, 5–16.

Kissin, S.A. and Owens, D.R. (1986) The properties and modulated structure of potosiite from the Cassier District, British Colombia. Canadian Mineralogist, 24, 45–50.

Li, J., Huang, J., Zhou, K., and Guilan, Z. (1988) An experimental study on three quarternary phases in the Fe-Sn-Sb-S system: Pb-free franckeite, Pb-free Cylindrite, and (Fe,Sb)-Ottemannite ss. Acta Geologica Sinica, 1, 4, 393–405.

Li, J. (1990) Die polymetallischen kassiterit-sulfiderz-paragenesen von dachang/China unter besonderer berücksichtigung oler sulfosalze. PhD Thesis (in German), University of Heidelberg

Ma, Z., Zhao, X., and Shi, N. (1997) STM study of franckeite surface. Acta Petrologica et Mineralogica, 16, 237–243.

Makovicky, E. (1976) Crystallography of cylindrite. Part I. Crystal lattices of cylindrite and incaite.Neues Jahrbuch für Mineralogie Abhandlungen, 126, 304–326.

Makovicky, E. and Hyde, B.G. (1992) Incommensurate, two-layer structures with complex crystal chemistry: Minerals and related synthetics. Materials Science Forum, 100-101, 1–100.

Organova, N.I., Dmitrik, A.L., and Laputina, I.P. (1980) On the structure of franckeite (in Russian) Geochem. and Mineral., Ref. Soviet Geol. At XXVI IGC, Nauka Moscow, 1980.

Stipp, S.L.S, Eggleston, C.M., and Nielsen, B.S. (1994) Calcite surface structure observed at micro-topographic and molecular scale with Atomic Force Microscopy (AFM). Geochimica et Cosmochimica Acta, 58, 3023–3033.

Stipp, S.L.S., Gutmannsbauer, W., and Lehmann, T. (1996) The dynamic nature of calcite surfaces in air. American Mineralogist, 81, 1–8.

Wang, S. (1989) Transmission electron microscope study of the minerals of the franckeite family. PhD Thesis (In Chinese). Chinese Geological University, Beijing, 1989.

Wang, S. and Kuo, K.H. (1991) Crystal lattices and crystal chemistry of cylindrite and franckeite. Acta Crystallographica, A47, 381–392.

Wang, S., Ma, Z.S., and Guo, K.X. (1992) An electron microscope study of mineral group of franckeite. Scientia Sinica, Series B: Chemistry, Life Sciences and Earth Sciences, 35, 6, 745–757.

Williams, T.B. and Hyde, B.G. (1988) Electron microscopy of cylindrite and franckeite. Physics and Chemistry of Minerals, 15, 521–544.

MANUSCRIPT RECEIVED DECEMBER 1, 2000
MANUSCRIPT ACCEPTED JUNE 28, 2002
MANUSCRIPT HANDLED BY H.W. NESBITT